Dynamic Response and Collapse of Slender Guyed Booms for Space Application

J.M. Housner* and W.K. Belvin*
NASA Langley Research Center, Hampton, Virginia

An analytical and experimental investigation of the nonlinear transient response of eccentric guyed slender booms with tip mass has been performed. The behavior of an experimental model is shown to correlate well with the predicted responses. The analysis has been used to study the transient response associated with slewing maneuvers of such structures in space and to develop an appropriate scaling law for model testing. Both applied step loads of finite duration and imposed initial velocities have been used to approximate transient conditions. Nonlinearities arising from cable slackening, beam-column behavior, and large geometry changes have been incorporated. Dynamic buckling of the boom is possible under excitations that result in cable slackening. Sensitivity to boom lateral eccentricities also has been considered. Transverse boom tip deflections are sensitive to initial eccentricities only when these eccentricities exceed certain threshold values. The nonlinear analysis also has been used to establish design guidelines for combinations of pulse level and duration that meet allowable deflection performance requirements.

Nomenclature

A_i = cross-sectional area of ith member

$\bar{c}_{cr}$ = $2\left[\sum_{i=1}^{3}\omega_{ei}^2(\sin^2\theta_i+\epsilon_i^*\cos^2\theta_i)\times(\bar{m}_n+\bar{m}_1/3+\bar{m}_2/3)\right]^{1/2}$ = critical damping value associated with ζ motion

$\bar{c}_\eta,\bar{c}_\xi,\bar{c}_{ik}$ = damping coefficient associated with η,ξ or f_{ik} generalized coordinates, respectively

e_{ik} = kth component of eccentricity in ith member

E_i = Young's modulus of ith member

f_{ik} = amplitude of kth flexural shape in ith member

F = lateral applied tip force

$\bar{g}_b,\bar{h}_b$ = frequency dependent functions given by Eq. (2b)

I_i = cross-sectional bending moment of inertia in ith member

J = mass moment of inertia about center of gravity

K = total number of sinusoidal components used to approximate flexural deformation

L_i = length of ith member

m_b,m_c,m_n = boom, cable, and tip mass, respectively

$\bar{m}_c$ = m_c/m_b

$\bar{m}_n$ = m_n/m_b

P_i^*,P_i = initial and time-varying average axial loads in ith member, respectively

$\bar{P}$ = ratio of boom initial compressive load to Euler load

$\bar{r}_i$ = ratio of radius of gyration to length of ith member

t = time

ϵ_i^*,ϵ_i = initial and time-varying average axial strains of ith member, respectively

η,ξ = axial and lateral boom tip motions

θ_i = initial angular location of ith member

$\bar{\lambda}_{1b},\bar{\lambda}_{2b}$ = dimensionless wavelength parameters defined in Eq. (2b)

τ = dimensionless time, Eq. (5f)

ω = circular frequency

ω_c = pinned-pinned cable frequency

$\bar{\omega}_{ei}$ = $[(E_iA_i/L_i)/m_b\omega_c^2]^{1/2}$

$\bar{\omega}$ = ω/ω_c

$\bar{\Omega}$ = dimensionless frequency, Eq. (2b)

Superscripts

$(\bar{\ })$ = dimensionless values

s,a = scaled and actual dimensions, respectively

Subscripts

a = attached tip mass

b,c = boom- or cable-related quantities

e = extensional property

i = cables, = 1 and 2; boom, = 3

Introduction

THERE is considerable interest in the development of lightweight structures for space application. Often such structures employ booms as one of their components. For example, slender and flexible booms are employed as feed masts in large antennas or to support solar panels on space stations. On Earth, slender flexible booms are often stiffened by external tension members, such as in guyed towers. Such a design possibility also exists for space applications with the external guys (or cables) adding little weight penalty.[1] Unlike Earth-bound guyed booms, those in space may be subjected to slewing maneuvers in which the whole space structure or just the guyed boom itself is rotated. These maneuvers excite vibrations of the boom and can lead to nonlinear effects due to large deformations. One such effect is slackening of the pretensioned guys (or cables). The effect of cable slackening on steady-state nonlinear vibrations of pretensioned structures was observed in Ref. 2 and considered in detail in Ref. 3. In addition, the loss of guy stiffness due to slackening can lead to a condition of instability resulting in the collapse of the boom.

The purpose of this paper is to present the development and application of an analysis for the nonlinear transient response of an initially imperfect slender guyed boom having a concentrated mass at the tip. The analysis is compared to laboratory experiments to confirm validity, and the validated analysis is employed to study the nonlinear transient boom response due to slewing maneuvers.

Presented as Paper 83-0821 at the AIAA/ASME/ASCE/AHS 24th Structures, Structural Dynamics and Materials Conference, Lake Tahoe, NV, May 2-4, 1983; submitted Jan. 18, 1984; revision received Jan. 21, 1985. This paper is declared a work of the U.S. Government and therefore is in the public domain.

*Aerospace Engineer, Structural Dynamics Branch, Structures and Dynamics Division.

During a slewing maneuver, the boom experiences transient loads at the initiation and termination of the maneuver. These loads may be approximated by a step pulse applied to the boom tip. For a step force of finite duration, design guidelines are established for allowable combinations of force level and duration that meet given performance requirements. Another approximation to the transient condition resulting from a slewing maneuver is an imposed initial velocity state that is proportional to the distance from the boom root. The initial velocity condition represents a sudden initiation or termination of a maneuver involving boom rotation. The imposed initial velocity conditions and the effect of boom eccentricities are also addressed.

Analysis

Linear Vibrations

Figure 1 depicts an eccentric boom supported by two pretensioned guys at one end and pinned to the ground at the other end. A linear analysis of the small vibrations of the guyed boom of Fig. 1 may be carried out using the exact element procedure of Ref. 3 and others.[4-6] The procedure is exact within the small vibrations theory of prestressed Euler-Bernoulli beams.

From Eq. (3) of Ref. 3, the linear vibrations of the guyed boom are governed by the transcendental frequency equation

$$\sum_{i=1}^{3}\{[P_i^* g_i + (EI)_i h_i]\cos^2\theta_i + (EA/L)_i \sin^2\theta_i\} - \omega^2 m_n = 0 \tag{1}$$

where summation is over the three elements (two cables and one boom), ω is the circular frequency, m_n the value of lumped mass at the boom tip, P_i^* the initial force in the ith member (positive for tension), and $\bar{g}_i$ and $\bar{h}_i$ are frequency-dependent quantities defined from the characteristic equation associated with the ith member.[3]

Equation (1) may be expressed in a dimensionless form as

$$\bar{h}_b - \pi^2 \bar{P}\bar{g}_b + \pi\bar{\Omega}\sqrt{2\bar{P}\bar{m}_c}\cos^2\theta/\tan\bar{\lambda}_c + \pi^4\bar{\omega}_e^2\bar{P}\sin^2\theta/\bar{m}_c - \bar{\Omega}^2\bar{m}_n = 0 \tag{2a}$$

where

$$\bar{g}_b = \bar{\lambda}_{1b}[1+(\bar{\lambda}_{1b}/\bar{\lambda}_{2b})\tan\bar{\lambda}_{1b}\coth\bar{\lambda}_{2b}] \times \{[1+(\bar{\lambda}_{1b}/\bar{\lambda}_{2b})^2]\tan\bar{\lambda}_{1b}\}^{-1}$$

$$\bar{h}_b = \bar{\lambda}_{1b}^3[1-(\bar{\lambda}_{1b}/\bar{\lambda}_{2b})\tan\bar{\lambda}_{1b}\coth\bar{\lambda}_{2b}] \times \{[1+(\bar{\lambda}_{1b}/\bar{\lambda}_{2b})^2]\tan\bar{\lambda}_{1b}\}^{-1}$$

$$\bar{\lambda}_{1b}^2 = \pi^2\bar{P}/2 + \sqrt{\bar{\Omega}^2 + \pi^4\bar{P}^2/4}$$

$$\bar{\lambda}_{2b}^2 = -\pi^2\bar{P}/2 + \sqrt{\bar{\Omega}^2 + \pi^4\bar{P}^2/4}$$

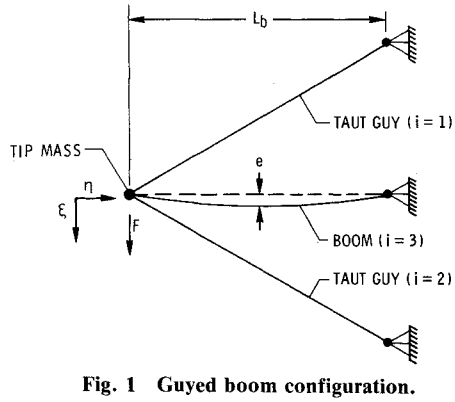

Fig. 1 Guyed boom configuration.

$$\bar{\lambda}_c = \pi\bar{\omega}; \qquad \bar{\omega}_e^2 = (EA/L)_c/m_b\omega_c^2$$

$$\omega_c^2 = \pi P_c/L_c m_c; \qquad \bar{P} = -P_b^*/P_E$$

$$\bar{\Omega}^2 = m_b L_b^3\omega^2/EI = \pi^4\bar{P}\bar{\omega}^2/2\bar{m}_c \tag{2b}$$

Subscripts c and b denote cable- or boom-related properties, respectively, and P_E is the Euler buckling load of the boom.

The third term of Eq. (2a) represents the effect of distributed cable inertia and is negligible when $\bar{m}_c$ is small. This term gives rise to system modes that involve cable vibration only. Because of the nondimensionalization, the cable modes lie at integer values of $\bar{\omega}$. When the boom bending stiffness increases without bound, $\bar{P}$ approaches zero and it can be shown that $\bar{\omega}$ approaches the frequency of a rigid boom pinned at one end and supported by springs at the other end. This frequency is denoted as the "pendulum frequency" and is given by

$$\bar{\omega}_p^2 = 6\bar{\omega}_e^2\sin^2\theta[1+2\bar{m}_c+3\bar{m}_n] \tag{3}$$

where

$$\bar{\omega}_p = \omega_p/\omega_c$$

The pendulum frequency may be compared to the lowest cable frequency $\bar{\omega}=1$, and to the lowest boom bending frequency, namely,

$$\bar{\omega}_b^2 = 2\bar{m}_c(1-\bar{P})/\bar{P} \tag{4}$$

where

$$\bar{\omega}_b = \omega_b/\omega_c$$

It may be shown that the guyed boom is statically unstable if either

$$\bar{P} \geq 1 \quad \text{or} \quad \pi^2\bar{\omega}_e^2\sin^2\theta/\bar{m}_c + \cos^2\theta \leq 1$$

The first condition represents Euler buckling of the boom, while the second represents a pendulum mode instability.

Some typical variations of frequency with $\bar{P}$ are shown in Fig. 2 for a guyed boom system where the pendulum frequency is greater than the first cable frequency. As the boom slenderness increases, $\bar{P}$ increases and the pendulum modes couples with the first boom bending mode yielding a frequency below the cable value. The value of $\bar{P}$ need not be very large for the pendulum-coupled first boom mode to become the fundamental mode of the system. A similar coupling occurs for higher boom- and pendulum-type modes.

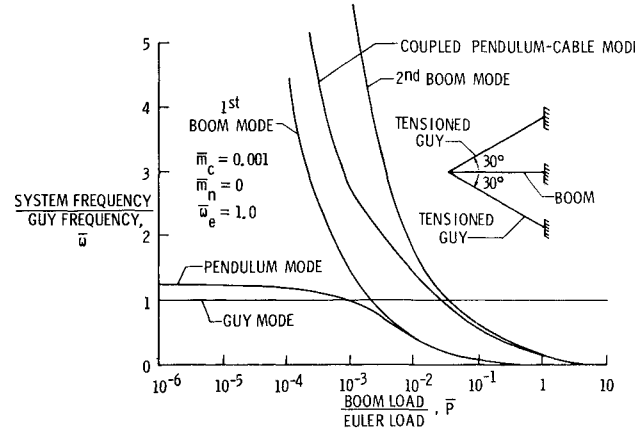

Fig. 2 Variation of linear natural frequency with compressive load parameter.

Large-Amplitude Nonlinear Transient Motion

The large-amplitude nonlinear transient motion is determined by using the equations of motion and time integration of Ref. 3. In dimensionless form, the three equations of motion are:

$$\sum_{i=1}^{3}\{\bar{L}_i\bar{\omega}_{ei}^2\epsilon_i[-\cos\theta_i+(\bar{\eta}/\bar{L}_i)\sin^2\theta_i-\tfrac{1}{2}(\bar{\xi}/\bar{L}_i)\sin 2\theta_i]+\bar{m}_i(\bar{\eta}''/3-\sin\theta_i\sum_{k=1}^{K}\bar{f}_{ik}''/k\pi)\}+\bar{c}_\eta\bar{\eta}'+\bar{m}_n\bar{\eta}''=0 \quad (5a)$$

$$\sum_{i=1}^{3}\{\bar{L}_i\bar{\omega}_{ei}^2\epsilon_i[-\sin\theta_i+(\bar{\xi}/\bar{L}_i)\cos^2\theta_i-\tfrac{1}{2}(\bar{\eta}/\bar{L}_i)\sin 2\theta_i]+\bar{m}_i(\bar{\xi}''/3+\cos\theta_i\sum_{k=1}^{K}f_{ik}''/k\pi)\}+\bar{c}_\xi\bar{\xi}'+\bar{m}_n\bar{\xi}''=\bar{F} \quad (5b)$$

$$\tfrac{1}{2}k^2\pi^2\bar{\omega}_{ei}^2\epsilon_i(\bar{f}_{ik}-\bar{e}_{ik})+(\bar{m}_i/k\pi)(\bar{\xi}''\cos\theta_i-\bar{\eta}''\sin\theta_i)+\tfrac{1}{2}\bar{m}_i\bar{f}_{ik}''+\bar{c}_{ik}\bar{f}_{ik}'+\tfrac{1}{2}k^4\pi^4\bar{r}^2\bar{\omega}_{ei}^2\bar{f}_{ik}=0$$

$$i=1,2,3; \quad k=1,2,\ldots,K \quad (5c)$$

where

$$\epsilon_i=\epsilon_i^*-(\bar{\eta}/\bar{L}_i)\cos\theta_i-(\bar{\xi}/\bar{L}_i)\sin\theta_i+(\pi^2/4\bar{L}_i^2)\sum_{k=1}^{K}k^2(\bar{f}_{ik}^2-\bar{e}_{ik}^2)+\tfrac{1}{2}(\bar{\eta}/\bar{L}_i)^2\sin\theta_i+\tfrac{1}{2}(\bar{\xi}/\bar{L}_i)^2\cos\theta_i-\tfrac{1}{2}(\bar{\eta}\bar{\xi}/\bar{L}_i)\sin 2\theta_i \quad (5d)$$

$$\bar{\eta}=\eta/L_b; \quad \bar{\xi}=\xi/L_b; \quad \bar{f}_{ik}=f_{ik}/L_b$$

$$\bar{e}_{ik}=e_{ik}/L_b; \quad \bar{L}_i=L_i/L_b; \quad \bar{r}_i=r_i/L_b$$

$$\bar{m}_i=m_i/m_b; \quad \bar{F}=F/(L_bm_b\omega_c^2) \quad (5e)$$

Primes denote differentiation with respect to dimensionless time τ, where

$$\tau=\omega_c t \quad (5f)$$

Equations (5a) and (5b) represent equilibrium in the $\bar{\eta}$ and $\bar{\xi}$ directions, respectively, while Eq. (5c) represents equilibrium in the generalized coordinate, $\bar{f}_{ik}$. The nonlinear equations (5a-c) are used to establish the scaling law given in the Appendix.

Nonlinear Effects

One nonlinear effect on the guyed boom response is the slackening of a cable. When the load in a cable vanishes, it is usually said that the cable is slack and has lost its stiffness both axially and laterally. There are two procedures for treating the possibility of slackening during a dynamic event. One procedure is approximate and involves removal of the stiffness and possibly the mass of a cable from the analysis when the cable load vanishes. In practice this procedure typically uses only the linear terms in determining whether a cable should be removed. The vanishing of the cable load is seen [Eq. (5d)] to be nonlinearly dependent upon the lateral deformation state of the cable. Consequently, the lateral deflections of the cable also are ignored in this procedure.

An alternate procedure is to retain the slackened cable and its associated kinetic energy, allowing it to lose its stiffness by the natural folding-up process incumbent upon it at slackening. In this procedure the cable load never actually vanishes, but approaches zero. This second procedure is clearly much more involved and computationally costly than the first since it requires modeling the cable in such a way as to allow it to fold up. In a previous paper,[3] the authors studied the relative merits of each approach on simple structural systems. Extrapolation of the conclusions of Ref. 3 to the present study implies that the first and less costly procedure is sufficient provided the ratio of cable mass to effective boom tip mass is much less than unity. Results of the present investigation have confirmed this conclusion. In the present study, the cable mass is retained during slackening and the stiffness is removed when the nonlinear strain [Eq. (5d)] vanishes.

A second nonlinear effect on the guyed boom response is the dynamic buckling of the boom. The cables are pretensioned and the boom is initially compressed. Provided the lateral tip motions are small and the stiffnesses of the two cables are identical, the boom compressive load remains unchanged. When the lateral tip motion is sufficient to cause a cable to slacken, the boom compression increases from the initial value. The increased compression causes the boom to soften axially and laterally. The degree of softening will depend on the initial boom imperfections and inertial properties. Additional nonlinear effects arise due to geometry changes. Although included in the analysis, these are usually of secondary importance.

Experimental Verification

Test Specimen

To verify the analysis, at two-dimensional guyed boom was designed and constructed as shown in the photograph of Fig. 3 and the schematic of Fig. 4. The boom is 1.5 m long and the cables attach at 48.8-deg angles relative to the boom axes. The boom member was constructed from a rectangular aluminum bar 6.35 mm thick and 25.4 mm wide. Minimum bending stiffness is in the plane of the cables. The boom is pinned to the ground at the base and attached to two 1.00-mm-diam cables at the tip. Unidirectional graphite epoxy cables were used since linear stress-strain cable behavior was desired. The structural eccentricity at the boom center is 2.5 mm and the boom shape is assumed to be a half-sine wave. An additional eccentricity due to the weight of the boom is 7.4 mm, such that the effective initial imperfection is 9.9 mm. A summary of member properties is given in Table 1.

Instrumentation

Numerous quantities could have been measured to correlate with analysis, however, the most applicable to antenna structures are boom tip displacements. Both axial and lateral displacements can occur when the boom is loaded. Thus, a two-dimensional displacement transducer was required.

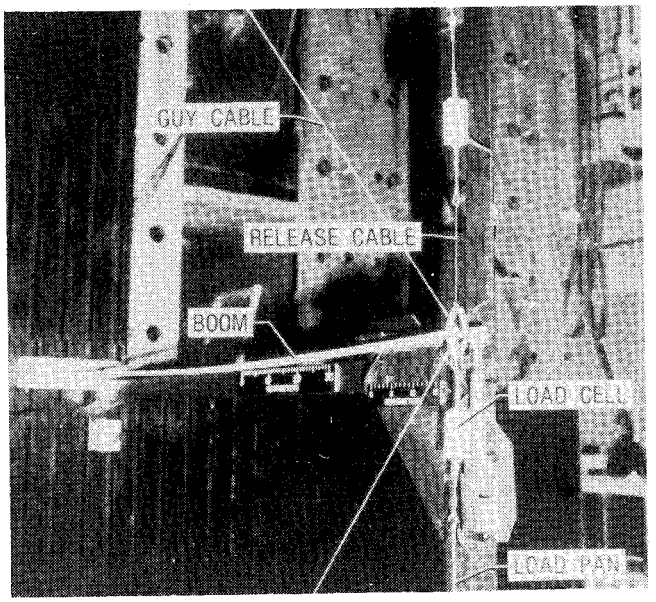

Fig. 3 Experimental setup.

Simultaneous measurement of both lateral and axial boom tip displacements was made with two direct-current differential transformers (DCDT) as shown in Fig. 4. The base of each DCDT was pinned to the ground, whereas the armature was pinned to the boom tip. This DCDT mounting procedure allowed the boom tip to rotate and translate freely. The lateral and axial motion was computed based on the law of cosines. The distances between the DCDT attachment points form a triangle of which one side remains constant. As the boom deflects, the change in the length of the other two sides of the triangle is measured. From this information, the law of cosines can be used to compute the absolute axial and lateral boom tip deflections.

In addition to displacement measurements, cable tension was measured by strain-gaged load cells in series with the cables. These load cells were attached near the root of the cable to reduce their inertial effects. Load cells were also used to measure the load applied to the guyed boom. All load and displacement measurements were recorded digitally at a sampling rate of 500 samples/s.

Test Procedure

Actuators used for station keeping and rigid-body controls in space may apply forces that closely approximate step loads of finite duration. A procedure was developed to simulate step load input into the experimental model as follows. Steel weights were attached to the load pan shown in Fig. 4. The model then deflected to the static equilibrium position. A release cable was used to return the boom to its undeflected position. The release cable was then severed and the structure was allowed to seek the new equilibrium position dynamically.

Since step loads are virtually impossible to produce, the actual applied load was measured so that it could be used in the analysis. The net applied load to the boom tip was measured by a load call in the release cable and a load cell in series with the load pan. The load cell in the release cable was necessary since it requires a finite time to release the cable. The resultant force from these two measurements is the applied load. Analytical response comparisons using a step load and the measured load indicate that this procedure closely simulates a step load.

Correlation

In this section, experimental and analytical correlations are presented. The analytical results are based upon the analysis presented herein. Static tests were performed to ensure the general accuracy of the test specimen material and geometric properties.

Table 1 Test specimen and instrumentation properties

Component	Mass, g
Boom, aluminum Length = 1.5 m, height = 6.35 mm, width = 25.4 mm	657.0
Cables, unidirectional graphite epoxy Diameter = 1.00 mm, length = 2.06 m[a]	
top cable measured $AE = 80.63\ E\ 3$N	2.55
bottom cable measured $AE = 83.67\ E\ 3$N	2.55
Instrumentation	
Load cells, length = 76.2 mm	78.2 ea
Displacement probes, nominal length = 200 mm ± 25.4 mm	105.0 ea
Fittings	
Turnbuckles, nominal length = 140 mm ± 50 mm	30 ea
Load pan attachment	21.1
Load pan	115.0

[a] Cables are in series with rigid turnbuckles and load cells.

Statics

Figure 5 displays the predicted and measured load deflection results for lateral and axial boom tip motion. Correlation is excellent. To simulate a static load in the dynamic analysis, a dynamic load was applied very slowly up to the desired level and then held constant. The resulting steady-state dynamic deflection was taken as the static value.

Dynamics

In general, the analysis used the measured force-time history of the experiment. A typical history is shown in Fig. 6 with an average load level of 111.2 N. It was produced by an applied 111.2 N weight in a fashion described in the test procedure section. Due 1) to the dynamics of the guyed boom and 2) to the load apparatus, the actual force oscillates about the 111.2 N loading as shown. Because the measured force includes the inertial effect of the weight, $\ddot{m}_n$ is set to zero when the measured force history is used in the analysis. However, when a pure step load is used in the analysis, $\ddot{m}_n$ is set to the appropriate value. As discussed in a later section, analytical predictions show that the response to the measured force is a good approximation to the response to a pure step load.

Dynamic Results in the Linear Range

For a nominal 22.23 N lateral tip force, cable slackening does not occur and, hence, the response remains in the linear range. Excellent correlation between experiment and analysis at this load level is shown in Fig. 7 for the boom tip lateral transient motion. Although not shown, axial motion at this load level is small. In comparison between experimental and analytical results, linear viscous damping with 5% of critical damping $\tilde{c}_{cr}$ associated with the ξ generalized degree of

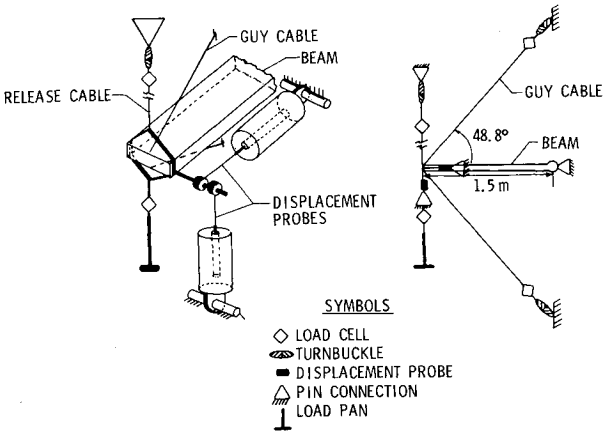

Fig. 4 Experimental model and instrumentation.

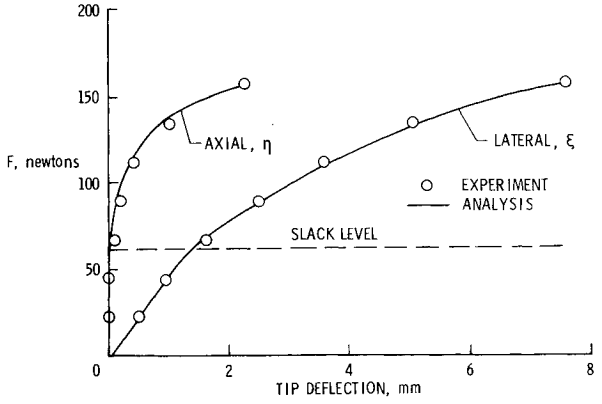

Fig. 5 Static load-deflection curves.

freedom was employed. This value was consistent with observed experimental free decay.

Dynamic Results in the Nonlinear Range

With increasing load level, the response assumes a nonlinear character. This is evident in Fig. 8 where the tip lateral and axial transient motions are displayed for a 111.2 N nominal lateral tip load. Both analysis and experiment reveal the nonlinear coupling of the lateral and axial motion. (This coupling is associated with the well-known nonlinear parametric resonance phenomenon.[7]) The axial tip motion is dominated by a frequency one-half the dominant lateral driving frequency. (See Fig. 6.) The lateral tip motion displays a combination of both the dominant driving frequency value and one-half its value, whereas in the linear range, Fig. 7, the lateral motion is dominated by the driving frequency only. Correlation is generally very good in the nonlinear range. However, the predicted peak amplitudes are 13-15% higher than the corresponding experimental amplitudes. This discrepancy may be attributed to one or a combination of factors associated with uncertainties in the experimental measurement, specimen properties, or nonlinear effects that are not accounted for, e.g., nonlinear damping. From Fig. 5 it is evident that in the large deflection range, small uncertainties in applied load can lead to large discrepancies in deflection.

Additional transient results, such as those of Fig. 8, were compiled at various load levels to form the composite results of Fig. 9. Here the measured and predicted peak tip responses are shown for increasing nominal load levels. The linear solution is also shown. Both measurement and analysis reveal a sharp deviation from the linear solution. Considering the difficulties involved in modeling transient motion in the nonlinear range, agreement is quite good.

Figure 10 displays the correlation between analytical results calculated using the measured applied load and those arrived at using a pure step load. Both loads give practically the same results and, consequently, the experimental load state is a reasonable approximation to a pure step load of the same average value.

Parameter Studies

Dynamic Load-Deflection Curves

The nonlinear analysis developed and validated herein was employed to study some of the basic response attributes of the guyed boom system. Figure 11 displays the variation in peak lateral tip deflection with both increasing levels of step load of infinite duration and slowly applied static load. The boom slenderness is 550 and the cables are pretensioned to compress the boom to 18% of the Euler load. Figure 11a contains results for a boom without a tip mass, while Fig. 11b contains results for a boom with tip mass equal to 10 times the boom mass. The tip mass may be envisioned as representing an antenna feed. In addition, Fig. 11 shows results for an initially straight boom ($e/L_b = 0$), and an imperfect boom with eccentricity ratio $e/L_b = -0.015$ when under no compressive load. The eccentricity is assumed to be in the form of a half-sine wave and increases from its nominal value when compressed by the pretensioned cables.

The static lateral load necessary to produce a slack cable and the static lateral load necessary to buckle the boom are indicated in the figures. For loads not exceeding the slackening load, the results are linear. Above slackening, they are highly nonlinear in the presence of the prescribed eccentricity ratio $e/L_b = -0.015$. The dynamic results always exceed the corresponding statically induced peak by a factor less than 2. Furthermore, eccentricity is seen to affect the lateral response peak significantly. However, the lateral sensitivity to imperfection appears to occur only when the imperfection exceeds a certain threshold value, as illustrated in Fig. 12. (This is not the case for axial motion which exhibits the usual sensitivity associated with axial compression of a beam column.) Note that the curve of Fig. 12 is not symmetric about the

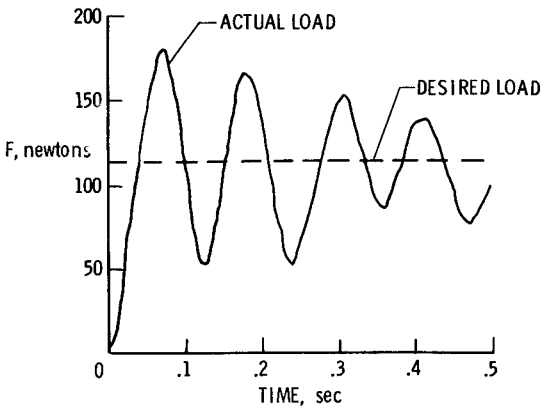

Fig. 6 Measured load between boom tip and load pan.

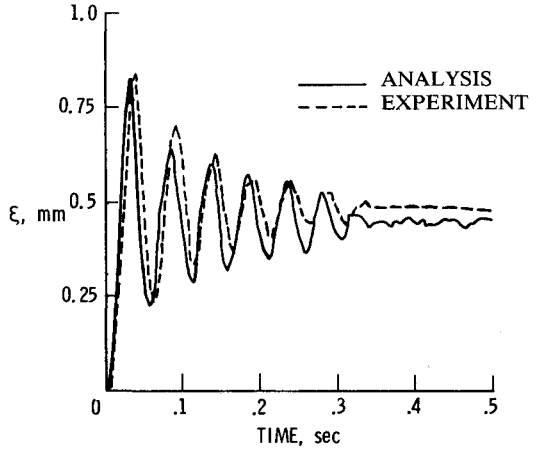

Fig. 7 Lateral tip deflection correlation in the linear range, $F = 22.22$ N.

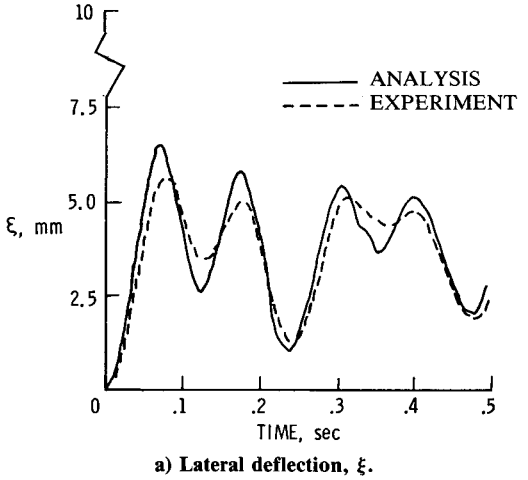

a) Lateral deflection, ξ.

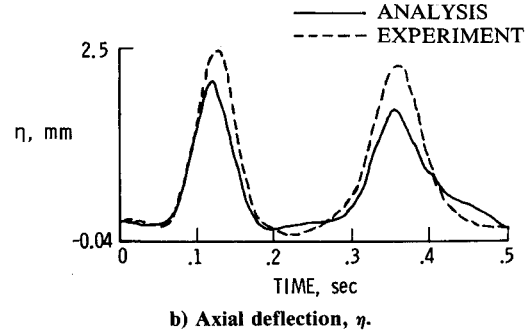

b) Axial deflection, η.

Fig. 8 Tip deflection correlation in the nonlinear range, $F = 111.1$ N.

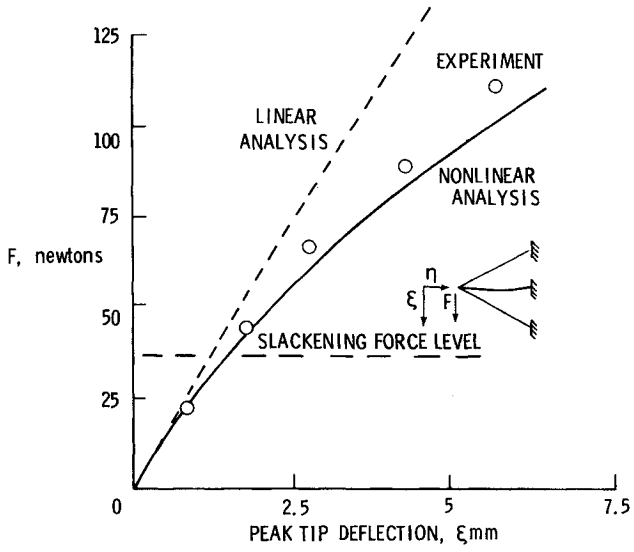

Fig. 9 Comparison of analytical peak lateral deflections at various load levels.

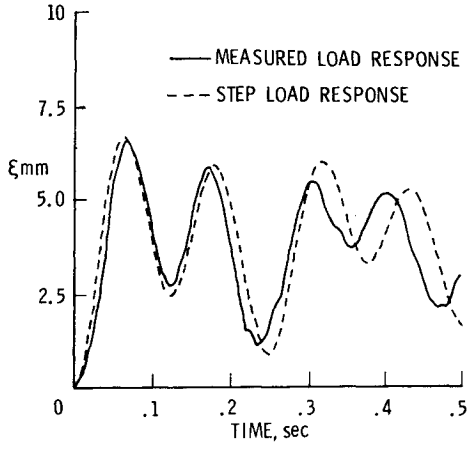

Fig. 10 Comparison of analytical responses due to step load and measured load.

perfect boom state. The asymmetry is a dynamic effect due to lateral inertial forces. The lateral tip deflections are greater when the eccentricity is in a direction opposite to the applied load.

The above-noted insensitivity of the lateral tip motion to small eccentricities implies that if high tolerances can be attained in guyed boom structures for space application, their lateral stiffness in the nonlinear range will only be significantly affected by cable slackening, and not beam-column behavior of the boom.

Effect of Pulse Duration

In the preceding studies, it has been assumed that the step load is of infinite duration. In practice, loads may have very short duration. This can have a profound effect on the response peak, since the peak under a step load of infinite duration may be reached after the actual load of finite duration has been removed. In this section an examination of the interaction between pulse level and load duration is made by determining the combination that results in a peak lateral tip motion less than a prescribed allowable value. Figure 13 contains two such interaction boundaries; one for no-tip-mass ratio and one for a tip-mass-to-boom-mass ratio of 10. To the left of each of these boundaries lie combinations of pulse level

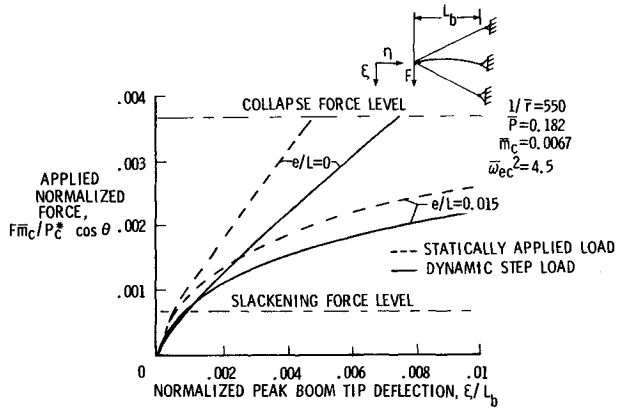

a) No tip mass, $\bar{m}_n = 0$.

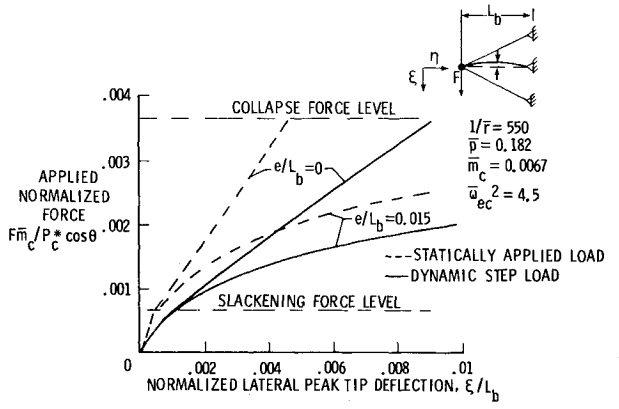

b) Tip mass, $\bar{m}_n = 10$.

Fig. 11 Variation of peak lateral tip deflection with applied step load.

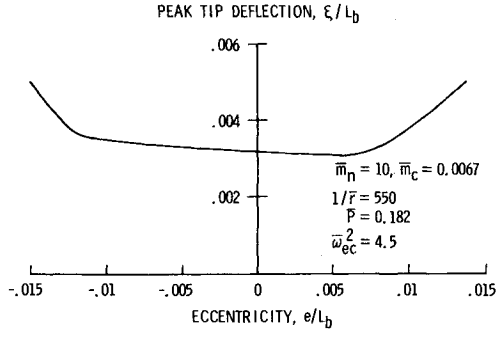

Fig. 12 Imperfection sensitivity of peak lateral tip deflection, $\bar{F} = 0.0015$.

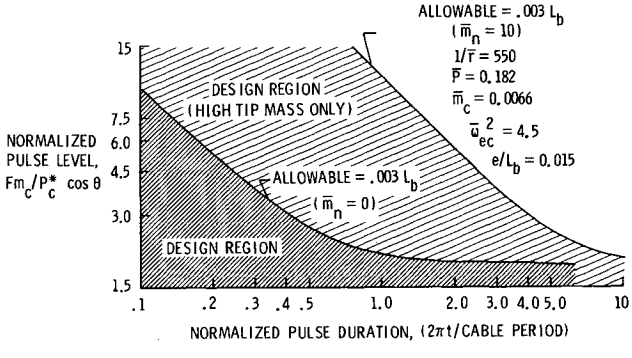

Fig. 13 Pulse duration design region due to a given performance requirement.

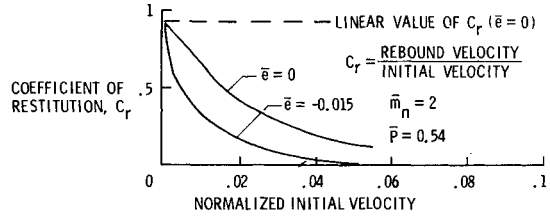

a) Variation of coefficient of restitution with normalized initial velocity from 0 to 0.1.

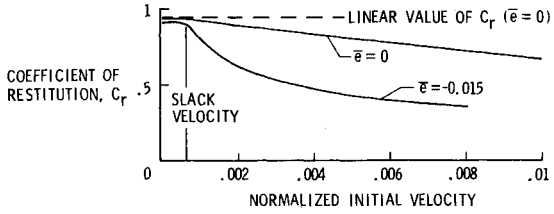

b) Enlargement of part (a) for low velocity from 0 to 0.01.

Fig. 14 Effect of initial velocity on guyed boom response.

and duration which result in tip deflections less than the allowable noted on the boundaries. Boundaries for other allowables can readily be generated by the analysis herein. Interaction curves such as those of Fig. 13 can provide guidelines in determining pulse level and duration to meet given performance requirements.

Initial Velocity Condition

In addition to examining the guyed boom response to an applied impulsive loading, it is also of interest to examine its response to an imposed initial velocity. The initial velocity condition may arise from the slewing maneuver of a primary structure with an attached boom. During a slewing maneuver, the boom is assumed to be moving initially as a rigid body with velocity varying linearly along its length. This is the pendulum mode shape. The primary structure is brought to a stop, but due to the boom flexibility, the boom tip continues moving.

As a consequence of the imposed initial velocity, the boom will vibrate. After one half cycle of motion the velocity amplitude of the boom tip or rebound velocity will be smaller than the initial tip velcoity. This is a result of damping and excitation of boom and cable modes which contain some of the initial kinetic energy of the system. The ratio of the magnitudes of rebound velocity to initial velocity, denoted as the coefficient of restitution, would be less than unity. If the system were linear, the coefficient of restitution would be independent of the initial velocity. Because the system is nonlinear, there will be considerable modal coupling and much of the initial kinetic energy in the pendulum mode will transfer into boom flexure. This results in the coefficient of restitution decreasing with increasing initial velocity.

Figure 14a illustrates the decrease of the coefficient below the linear value for a particular sample case. Figure 14b is an enlargement of Fig. 14a for low velocities. The line denoted "slack velocity" indicates the value of initial velocity which causes cable slackening. The figures reveal that the decrease from the linear value effectively begins once slackening is initiated. This is similar to what occurs in the presence of force loading. When the coefficient of restitution goes to zero, the system has collapsed.

Concluding Remarks

An analytical and experimental investigation of the nonlinear transient response of guyed slender space booms with tip mass has been performed. In general, correlation of the transient responses arising from applied pulses is very good, although the nonlinear analysis predicts somewhat higher peak deflections than experimental values in the nonlinear range. This discrepancy may be due to the occurrence of small uncertainties in load measurement that can lead to large deflection discrepancies at high dynamic load levels.

The analysis has been used to study the transient response of the system to suddenly applied step loads and prescribed initial velocities. Both cases approximate the transient conditions associated with commencing and terminating a slewing maneuver in space. Two significant nonlinear effects have been examined, namely, cable slackening and beam-column behavior. Dynamic buckling of the boom may occur with excitations that result in cable slackening. Sensitivity to boom imperfections has been considered as well. It appears that transverse boom tip deflections are sensitive only to initial eccentricities when certain threshold values are exceeded. The nonlinear analysis has also been used to establish design guidelines for combinations of pulse level and duration which meet performance requirements for allowable deflections. In addition, the nondimensional governing equations yield guidelines for scale-model construction and testing.

Appendix

Scaling Law Development

It is often desirable to construct and test scale models of aerospace structures. This is especially so in the area of space structures where the actual structure may span very large distances. The dimensionless form of the governing equations permits the development of a scaling law. The scaling law permits data obtained from the scale model to be translated to the actual structure.

It is assumed that the scale model is designed such that all of its dimensions are proportional to the actual article, i.e.,

$$L^{i(s)} = NL_i^{(a)} \tag{A1}$$

where N is a scale factor usually less than one and superscripts s and a refer to scaled and actual articles, respectively. The material properties of the scaled article are assumed to be the same as the actual article, thus, it follows that:

$$E^{(s)} = E^{(a)}; \quad m_i^{(s)} = N^3 m_i^{(a)}; \quad \omega_{ei}^{(s)} = \omega_{ei}^{(a)}/N; \quad \omega_c^{(s)} = \omega_c^{(a)}/N \tag{A2}$$

Further, it is assumed in constructing a scale model that one desires the model to have deflections proportional to the actual article through the scale factor N. Thus, it is desired that the dimensionless deflections of the scale model are identical to those of the actual article, i.e.,

$$\bar{\eta}^{(s)} = \bar{\eta}^{(a)}; \quad \bar{\xi}^{(s)} = \bar{\xi}^{(a)}; \quad \bar{f}_{ik}^{(s)} = \bar{f}_{ik}^{(a)} \tag{A3}$$

Consequently, all dimensionless physical quantities are unaffected by the scaling.

For a system such as the guyed boom, which is governed by nonlinear equations, this is the only practical choice. Thus, from Eqs. (5a-c) it is apparent that Eq. (6a) will be satisfied provided the applied dimensionless force scales as

$$\bar{F}^{(s)} = \bar{F}^{(a)} \tag{A4}$$

Then from Eq. (5e) one finally finds

$$F^{(s)} = N^2 F^{(a)} \tag{A5}$$

Scaling Law Summary

This scaling law calls for a scale model in which all dimensionless parameters are equal to those of the actual article. The deflections of the scale model will then be proportional to those of the actual article with proportionality constant N. Table A1 lists the scaling of all dimensional values.

Table A1 Scaling law

Quantity	Scale Factor = scaled value/actual value
Length	N
Area	N^2
Area moment of inertia	N^4
Mass	N^3
Mass moment of inertia	N^5
Frequency	$1/N$
Preload	N^2
Applied force	N^2
Applied torque	N^3
Deformation	N
Gradient	1
Curvature	$1/N$
Bending moment	N^3
Stress	1

Consequences of Scaling Law on Rigid-Body Rotations

For a rigid body, the rotations of the body are governed by

$$T^{(a)}/J^{(a)} = \ddot{\theta}^{(a)} \tag{A6}$$

where T and J denote torque and rotational inertia, respectively, about the system center of gravity and θ denotes a rigid-body rotation angle. If the system were not grounded, but attached to some body that was free in space, then the force relation of Eq. (A5) implies that

$$\ddot{\theta}^{(s)} = \ddot{\theta}^{(a)}/N^2 \tag{A7}$$

Thus, if a rigid scale model is tested free-free in a laboratory, the scaling of the applied forces required to produce scaled deflections on a deformable body would result in a scaled model with a slewing acceleration much greater than the actual since N is usually much smaller than unity.

It can also be shown that if one wishes to scale such that the rigid-body slewing motions in the actual and scale models are identical, then

$$F^{(s)} = N^4 F^{(a)} \tag{A8}$$

This would, of course, lead to extremely small structural deformations of the scale model and, due to the nonlinear nature of the governing structural equation, it would be quite difficult, if not impossible, to relate the structural deformations of the scale model back to the actual article.

References

[1]Russell, R.A., Campbell, T.G., and Freeland, R.E., "A Technology Development Program for Large Space Antennae," NASA TM-81902, Sept. 1980.

[2]Belvin, W.K., "Analytical and Experimental Vibration and Buckling Characteristics of a Pretensioned Stayed Column," *Journal of Spacecraft and Rockets,* Vol. 21, Sept.-Oct. 1984, pp. 456-462.

[3]Housner, J.M. and Belvin, W.K., "On the Analytical Modeling of the Nonlinear Vibrations of Pretensioned Space Structures," *Journal of Computers and Structures,* Vol. 16, 1983, pp. 339-352.

[4]Anderson, M.S., "Vibration of Prestressed Periodic Lattice Structures," *AIAA Journal,* Vol. 20, April 1982, pp. 551-555.

[5]Anderson, M.S., "Nonlinear and Tangent Stiffness of Imperfect Beam Columns," NASA TM 84497, Dec. 1982.

[6]Akesson, B.A., "A Computer Program for Space Frame Vibration Analyses by an Exact Method," *International Journal of Numerical Methods in Engineering,* 1976, pp. 1121-1231.

[7]Bolotin, V.V., *The Dynamic Stability of Elastic Systems,* Holden-Day Inc., San Francisco, CA, 1964, pp. 9-12, 29-32.